



## Facile one-pot hydrothermal synthesis and structural characterization of transition metals (Cu, Co and Mn) doped ZnS nanoparticles in HMTA matrix

K. Vijai Anand<sup>2,\*</sup>, R. Mohan<sup>3</sup>, R. Jayavel<sup>1,#</sup>

<sup>1</sup>Centre for Nanoscience and Technology, Anna University, Chennai-600 025, India.

<sup>2</sup>Department of Physics, Sathyabama University, Chennai-600 119, India.

<sup>3</sup>Department of Physics, Presidency College, Chennai-600 005, India.

Received 23 Feb 2015, Revised 08 Jan 2016, Accepted 19 Jan 2016

\* E-mail: [anandkvijai@yahoo.co.in](mailto:anandkvijai@yahoo.co.in) / [anandkvijai@gmail.com](mailto:anandkvijai@gmail.com) / # [rjvel@annauniv.edu](mailto:rjvel@annauniv.edu), Phone.: +91 44 24503150; Fax: +91 44 24502344

### Abstract

Transition metals (Cu, Co and Mn) doped ZnS nanoparticles have been prepared by a facile one-pot hydrothermal method using Hexamethylenetetramine (HMTA), a non-toxic surfactant in aqueous solution. The structural properties of the prepared samples were studied using XRD, TEM, SEM and FTIR analysis. X-ray diffraction (XRD) studies show that the average grain size of the prepared ZnS nanoparticles is around 2 nm with cubic zinc blende structure and doping of transition metals has no effect on the crystal structure. TEM results showed that the synthesized nanoparticles were uniformly dispersed in the HMTA matrix without aggregation. Formation of HMTA stabilized ZnS nanoparticles were confirmed by FTIR studies.

**Keywords:** Zinc sulfide, nanoparticles, transition metals, HMTA surfactant, hydrothermal

### 1. Introduction

Synthesis and study of nanostructured materials have become a major interdisciplinary area of research over the past few decades. Research on nanosized semiconductors stimulated great interest in recent years and showed great potential applications because of their unique properties such as unusual luminescence properties induced by quantum size effect [1]. Luminescent semiconductor nanoparticles are considered to be the materials for the next generation displays, bio-labels, lasers etc. due to their high luminescence quantum efficiency, spectral tunability, color purity, high optical gain with lower threshold and high chemical stability [2]. Among a variety of semiconducting materials, the binary metal chalcogenides of group II-VI semiconductors have been extensively used due to their potential applications owing to their non-linear optical properties, luminescent properties, quantum size effect and other important physical and chemical properties [3]. Doped metal chalcogenide nanostructured materials have attracted much attention due to their wide range of applications in light emitting displays, optical sensors, electroluminescence devices etc. This kind of nanomaterials exhibit unusual physical and chemical properties in comparison with their bulk materials, such as size dependent variation of the band gap energy. Furthermore, impurity ions doped into these nanostructures can influence the electronic structure and transition probabilities [4]. The doped semiconductor nanoparticles have also attracted great interest due to their characteristics such as short luminescence life-time, size independent emission color tunability, low-voltage cathodoluminescence and alternate-current electroluminescence [5]. As an important II-VI semiconductor material, ZnS is chemically more stable and technologically important than other chalcogenides. Hence, it is considered to be a promising host material with wide range of applications in light emitting displays, optical sensors, electroluminescence devices etc. Many methods such as hydrothermal, thermal evaporation, co-precipitation, micro emulsion etc. have been employed to prepare transition metals doped ZnS nanostructures [6-10]. Among these methods, hydrothermal method has been demonstrated to be a powerful tool to generate semiconductor nanostructures with high quality and monodispersity. This method is ideally suited for precise control of size and shape of nanomaterials. In addition, they save energy and are environmentally benign because the reactions take place in closed system conditions at low temperature.

During the chemical synthesis of nanoparticles, organic stabilizers are usually used to prevent them from aggregation by capping their surfaces. Moreover, the introduction of stabilizers also influences on the chemical and physical properties of semiconductor materials, from stability to solubility and to light emission [11]. Therefore, proper surface modification by stabilizers can significantly increase the quantum yield of the excitonic emission. On the other hand, the surface states will play a very important role in the nanoparticles, due to their large surface to volume ratio with a decrease in particle size. These quantum size effects have stimulated great interest in both basic and applied research [12]. There have been extensive reports in the past few years demonstrating the systematic exploration of growing ZnS nanoparticles in the surfactant system to control the particle size [13- 16]. Even though surfactant-assisted technique is an effective pathway for the preparation of nanoparticles, most of the commercial surfactants employed are hazardous chemical substances. Hence, it is necessary to adopt a more eco-friendly route for the preparation and passivation of the nanoparticles using a non-toxic surfactant. The hexamethylenetetramine (HMTA) surfactant is a non-toxic, water soluble and non-ionic tetradenate cyclic tertiary amine, which served not only as complexing or stabilizing agent but also as an indirect soft template. In our previous work, the structural, optical and thermal stability properties of HMTA capped ZnS nanoparticles has been studied [17-20]

In this present investigation, structural properties of transition metals (Cu, Co and Mn) doped ZnS nanoparticles prepared via a facile one-pot hydrothermal route using HMTA (Hexamethylenetetramine), a non-toxic surfactant were studied using various characterization techniques.

## 2. Experimental

### 2.1. Synthesis of HMTA stabilized pure and transition metals doped ZnS nanoparticles

HMTA stabilized pure ZnS nanoparticles were synthesized as per the procedure reported earlier [17]. In the case of HMTA stabilized transition metals (Cu, Co and Mn) doped ZnS nanoparticles, dihydrates of zinc, copper, cobalt and manganese acetate were mixed with Hexamethylenetetramine (HMTA) ( $C_6H_{12}N_4$ ) and thiosemicarbazide ( $CH_3N_3S$ ) along with sodium hydroxide (NaOH). The synthesis was carried out by adding zinc acetate dihydrate/thiosemicarbazide/HMTA/sodium hydroxide=0.95/1/0.5/0.5 (mole ratio) along with 0.05 M of copper acetate dihydrate ( $(CH_3COO)_2 Cu \cdot 2H_2O$ ) for Cu doped ZnS, 0.05 M of cobalt acetate dihydrate ( $(CH_3COO)_2 Co \cdot 2H_2O$ ) for Co doped ZnS and 0.05 M of manganese acetate dihydrate ( $(CH_3COO)_2 Mn \cdot 2H_2O$ ) for Mn doped ZnS in the Teflon-lined chamber, which was then filled with deionized water up to 80% of its volume. The closed chamber was placed inside a resistive heating furnace and heated at 180 °C for 8 h and then cooled down to room temperature. The resulting precipitate were filtered off and washed several times in distilled water and ethanol. The final products were dried in vacuum at 90 °C for 4 h.

### 2.2. Characterization of nanoparticles

The XRD patterns of the prepared samples were recorded with Siemens D-5005 X-ray powder diffractometer, using  $CuK_{\alpha}$  radiation ( $\lambda=1.5418 \text{ \AA}$ ). JEOL 3010 TEM studies reveal the morphology and size of the nanoparticles. SEM analyses were carried out by using Quanta FEG 200 SEM apparatus to study the surface features of pure and doped ZnS nanoparticles. FTIR spectra were recorded with Perkin Elmer RX1 Model FTIR spectrophotometer by KBr pellet method in the range 4000 to 500  $cm^{-1}$ .

## 3. Results and Discussion

### 3.1. X-ray diffraction (XRD) analysis

Powder X-ray diffraction (XRD) patterns for pure and transition metals (Cu, Co and Mn) doped ZnS nanoparticles are shown in Fig. 1. The patterns indicate that all the samples possess cubic zinc blende structure of ZnS (JCPDS file No. 05-0566) [21]. Diffraction peaks from (111), (220) and (311) planes alone appeared in the XRD pattern and all other high-angle peaks have submerged in the back ground due to the large line broadening, which is attributed to nanosize of the particles. No additional peaks were observed, indicating that within the resolution of XRD measurement, there were no structural changes and formation of additional phases due to the incorporation of transition metal dopants in ZnS. This confirms that the cubic phase of ZnS structure is not disturbed by the transition metals (Cu, Co and Mn) substitution. The XRD peaks of all the samples are quite similar, except a small shift in the peak positions, which may be due to the difference in the ion radii of the transition metal ( $Cu^{2+}$ ,  $Co^{2+}$  and  $Mn^{2+}$ ) compared to Zn. The variation of d-spacing with corresponding (hkl) planes for pure and transition metals (Cu, Co and Mn) doped ZnS samples are tabulated in Table 1. These values are consistent with the standard cubic phase of ZnS [22].

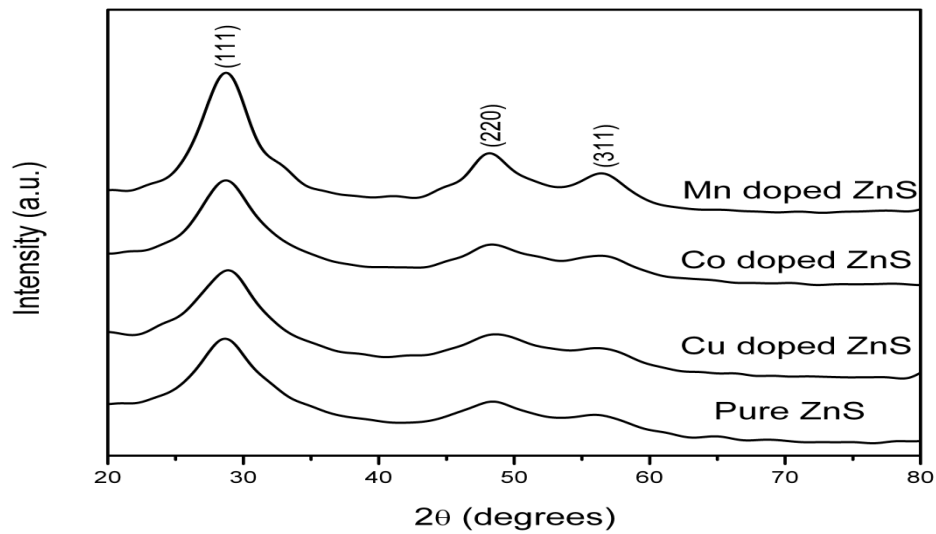


**Figure 1:** XRD patterns of HMTA stabilized pure and transition metals doped ZnS nanoparticles.

**Table 1.** Variation of d-spacing with corresponding (hkl) planes for pure and transition metals (Cu, Co and Mn) doped ZnS

Sample	Plane	$d_{hkl}$ (Å)	$a$ (Å)	$V$ (Å <sup>3</sup> )
Pure ZnS	(111)	3.13	5.40	158.02
	(220)	1.90		
	(311)	1.62		
Cu doped ZnS	(111)	3.11	5.36	154.18
	(220)	1.88		
	(311)	1.62		
Co doped ZnS	(111)	3.11	5.37	154.99
	(220)	1.89		
	(311)	1.62		
Mn doped ZnS	(111)	3.12	5.38	155.72
	(220)	1.89		
	(311)	1.62		

From Table 1, the lattice parameters decrease for transition metals (Cu, Co and Mn) doped ZnS nanoparticles compared to pure ZnS nanoparticles. The average grain size of pure and transition metals (Cu, Co and Mn) doped ZnS nanoparticles are approximately 1.75 nm, 1.95 nm, 1.98 nm and 2.05 nm respectively, which are calculated from the full width at half-maximum (FWHM) of the most intense peak using the Scherrer's formula[23]:

$$D = \frac{0.9 \lambda}{\beta \cos \theta} \quad (1)$$

where  $\lambda$  is the wavelength of the X-ray radiation (for  $\text{CuK}_\alpha$  radiation,  $\lambda = 1.5418 \text{ \AA}$ ),  $\beta$  is the FWHM in radians of the XRD peak and  $\theta$  is the angle of diffraction.

### 3.2. Transmission electron microscope (TEM) and Selected area electron diffraction (SAED) studies

The morphology and size of HMTA stabilized pure and transition metals doped ZnS nanoparticles were studied using TEM. Fig. 2 shows a high-magnification TEM image of HMTA stabilized (a) pure and (b, c) Co doped ZnS samples, which indicate that the sample is composed of large quantity of well-dispersed spherical nanoparticles with uniform size and shape. The average size of these particles estimated from the TEM image is

about 2 nm, which is in good agreement with the results obtained from X-ray diffraction (XRD) analysis. The selected-area electron diffraction (SAED) pattern of HMTA stabilized Co doped ZnS nanoparticles (Fig. 2(d)) shows a set of concentric rings instead of sharp spots due to the random orientation of the crystallites, which relate to diffraction from different planes of the ZnS nanocrystallites [24]. The diffraction rings are indexed to (111), (220) and (311) planes of the cubic ZnS phase (JCPDS File No. 05-0566) [18].

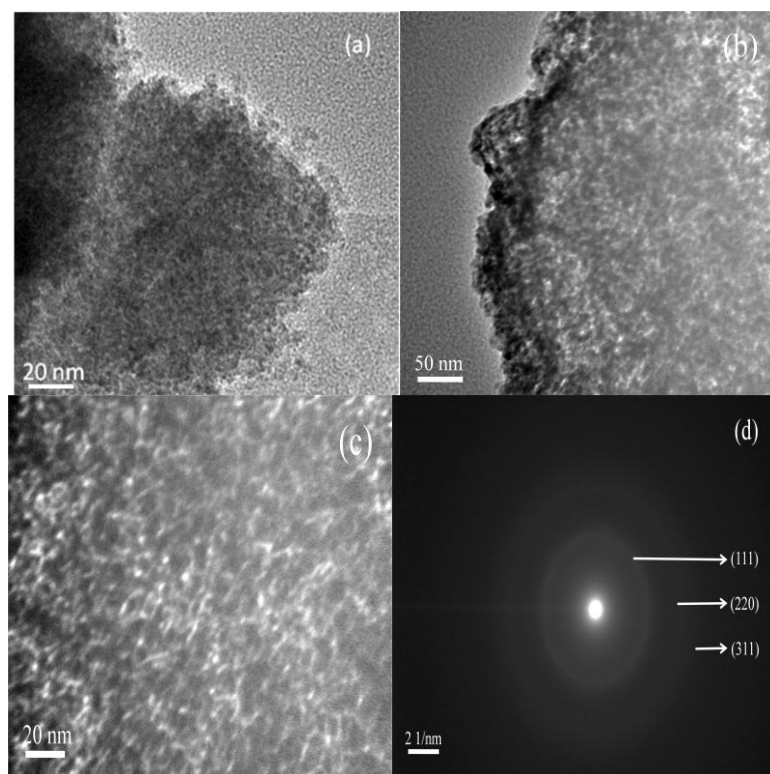


**Figure 2:** TEM images of HMTA stabilized (a) pure, (b, c) Co doped ZnS nanoparticles and (d) SAED pattern of Co doped ZnS nanoparticles.

### 3.3. Scanning electron microscope (SEM) studies

SEM micrographs of HMTA stabilized pure and transition metals (Cu, Co and Mn) doped ZnS samples are shown in Fig. 3(a-d). From the SEM image, it is clear that the particles were uniformly distributed with spherical morphology.

### 3.4. Fourier transform infrared spectroscopy (FTIR) studies

Fig. 4 depicts the FTIR transmission spectra of (a) HMTA, (b) HMTA stabilized pure and (c-e) transition metals (Cu, Co and Mn) doped ZnS nanoparticles. It is to be noted that all the absorption peaks of HMTA in Fig. 4(a), matches with those reported in the literature [25]. The sharp peak in all the samples at around  $2358\text{ cm}^{-1}$  is due to carbon. The spectrum (Fig. 4(a)) reveals the C-H stretching vibration bands at  $2920\text{ cm}^{-1}$ , the C-H bending modes at  $1487\text{ cm}^{-1}$  and the relatively weak methylene rocking vibration at  $690\text{ cm}^{-1}$ . The vibration at  $690\text{ cm}^{-1}$  is characteristic of a minimum of four methyl groups,  $(\text{CH}_2)_4$  in a row and assigned to the methylene rocking vibration. Hence, it is concluded that the long alkyl chain does exist in HMTA [26]. A peak due to the stretching vibrations of C-H bonds in tertiary amines of HMTA at  $1006\text{ cm}^{-1}$  was observed in the vibrational spectra [27]. The absorption peaks at  $3312$  and  $3489\text{ cm}^{-1}$  are assigned due to O-H stretching vibrations. The absorption peaks at  $3407$  and  $1601\text{ cm}^{-1}$  in the Fig. 4 (b) are assigned to water molecule and hydrogen bonded hydroxyl groups respectively. The absorption peak at  $2078\text{ cm}^{-1}$  may be from the decomposition product of thiosemicarbazide during the synthesis of ZnS nanoparticles. Other peaks observed at  $2925$ ,  $1494$ ,  $1375$  and  $1091\text{ cm}^{-1}$  correspond to C-H bonding, due to the formation of co-ordination bond between the nitrogen atom of the HMTA and  $\text{Zn}^{2+}$  ions [28]. Hence, capping of ZnS nanoparticles with HMTA molecules is confirmed. The weak peaks observed at  $2865$  and  $2925\text{ cm}^{-1}$  are assigned to symmetric and asymmetric C-H stretching.

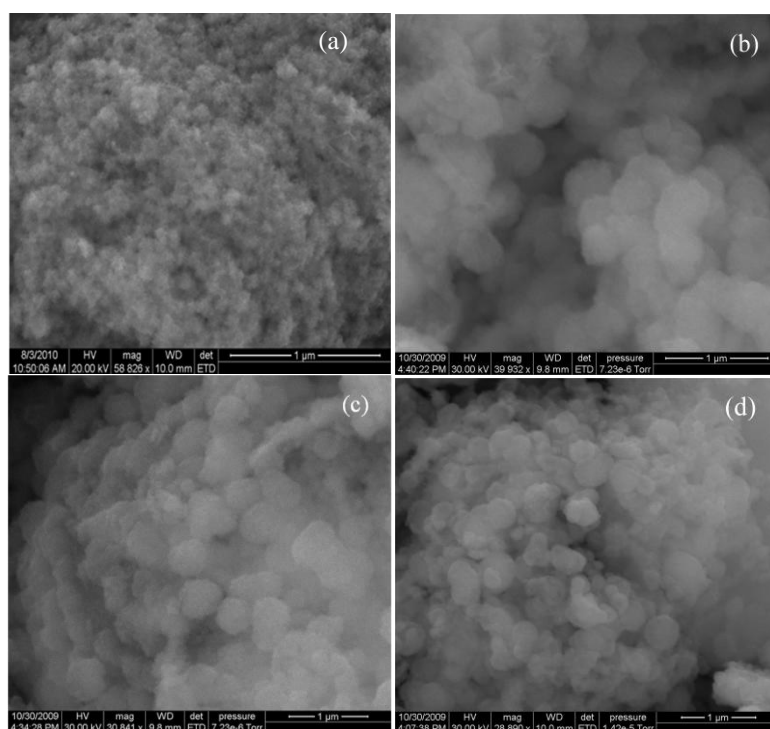


**Figure 3:** SEM micrographs of HMTA stabilized (a) pure (b) Cu doped (c) Co doped and (d) Mn doped ZnS nanoparticles.

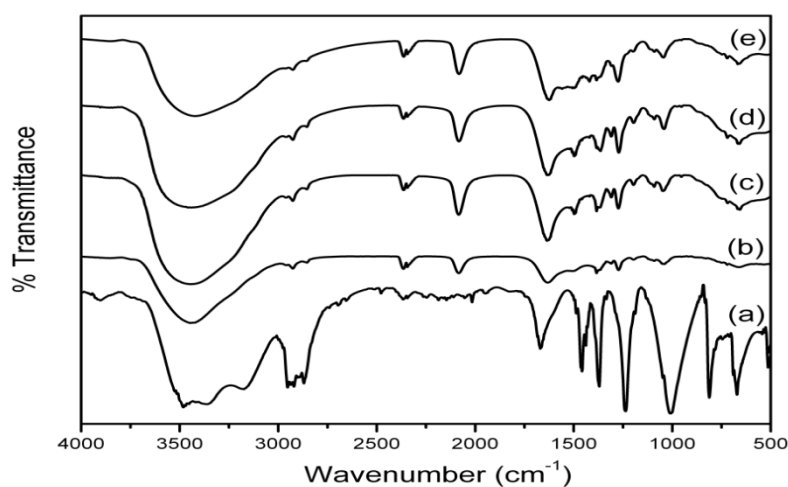


**Figure 4:** FTIR transmission spectra of (a) HMTA (b) HMTA stabilized pure (c) Cu doped (d) Co doped and (e) Mn doped ZnS nanoparticles.

The C-H bonds are present in the monoacetate groups as an intermediate product. The peak at  $659\text{ cm}^{-1}$  is assigned to the Zn-S stretching vibration and ZnS band, which corresponds to sulfides [29]. Bands around  $3000 - 3600\text{ cm}^{-1}$  are due to the hydrogen stretching frequency (OH Stretching) and bands around  $900 - 1500\text{ cm}^{-1}$  are due to the oxygen stretching and bending frequencies. Bands at around  $1270$  and  $1100\text{ cm}^{-1}$  are due to the characteristic frequency of inorganic ions. Weak additional bands were observed at  $754$ ,  $884$  and  $950\text{ cm}^{-1}$ , indicative of the presence of resonance interaction between vibrational modes of sulfide ions [30]. The C-N stretching vibrations at frequency below  $1000\text{ cm}^{-1}$  are shifted towards lower frequency, which might result from the chemical bonding between  $\text{Zn}^{2+}$  and N atom. In addition, at frequency above  $1200\text{ cm}^{-1}$ , the IR spectrum of HMTA stabilized ZnS nanoparticles exhibit different peaks compared to pure HMTA spectrum, which may be due to the ordered alignment and regular confirmation of  $(\text{CH}_2)_6\text{N}_4$  molecules in the final product. Thus, it is evident from FTIR spectra that, when the passivating agent (HMTA) encapsulates the ZnS nanoparticles, a shift in the absorption peak is observed, indicating the process of capping being done successfully.

For the Cu doped ZnS nanoparticles (Fig. 4(c)), the absorption peaks at 2927, 2853, 1492, 1377 and 1041  $\text{cm}^{-1}$  are attributed to C-H bonding and other peaks observed at 3445 and 658  $\text{cm}^{-1}$  are due to O-H stretching and Zn-S stretching vibrations. In the case of Co doped ZnS nanoparticles (Fig. 4(d)), the absorption bands at 2925, 2863, 1494, 1370 and 1040  $\text{cm}^{-1}$  are assigned to C-H bonding and other peaks at 3450 and 656  $\text{cm}^{-1}$  are due to O-H stretching and Zn-S stretching vibrations. In the Mn doped ZnS nanoparticles (Fig. 4(e)), the absorption peaks at 2929, 2861, 1492, 1385 and 1049  $\text{cm}^{-1}$  are mainly due to C-H bonding, whereas the peaks at 3427 and 660  $\text{cm}^{-1}$  are attributed to O-H stretching and Zn-S stretching vibrations.

## Conclusion

A facile one-pot hydrothermal method has been adopted for the synthesis of transition metals (Cu, Co and Mn) doped ZnS nanoparticles using hexamethylenetetramine (HMTA) as a surfactant in aqueous solution. The crystal structure and average grain size of the HMTA stabilized ZnS samples were determined by XRD analysis. The TEM image shows that the HMTA stabilized ZnS nanocrystalline size is around 2 nm and is in good agreement with the particle size estimated from the XRD analysis. The presence of HMTA over the prepared ZnS samples was confirmed by FTIR studies.

## Acknowledgements

TEM and SEM facilities provided by SAIF, Indian Institute of Technology, Chennai are gratefully acknowledged.

## References

1. Wang M., Sun L., Fu X., Liao C., Yan C., *Solid State Comm.* 115 (2000) 493
2. Manzoor K., Aditya V., Vadera SR., Kumar N., Kutty TRN., *J. Phys. Chem. Solids* 66(7) (2005) 1164.
3. Nanda J., Sarma DD., *J. Appl. Phys.* 90 (2001) 2504.
4. Peng WQ., Cong GW., Qu SC., Wang ZG., *Opt. Mater.* 29 (2006) 313.
5. Bhargava RN., Gallagher D., *Phys. Rev. Lett.* 72 (1994) 416.
6. Khosravi AA., Kundu M., Jatwa L., DeshpandeSK., Bhagwat UA., Sastry M., Kulkarni SK., *Appl. Phys. Lett.* 67 (1995) 2702.
7. Lee S., Song D., Kim D., Lee J., Kim S., Park IY., Choi UD. *Mater. Lett.* 58 (2004) 342.
8. Ren G., Lin Z., Wang C., Liu W., Zhang J., Huang F., Liang J. *Nanotechnology* 18 (2007) 035705.
9. Bhattacharjee B., Ganguli D., Iakoubouskii K., Stesmans A., Chaudhuri S. *Bull. Mater. Sci.* 25 (2002) 175.
10. Geng B.Y., Zhang L.D., Wang G.Z., Xie T., Zhang Y.G., Meng G.W., *Appl. Phys. Lett.* 84 (2004) 2157.
11. Tang H., Yan M., Zhang H., Xia M., Yang D., *Mater. Lett.* 59(8-9) (2005) 1024.
12. Henglein A., *Chem. Rev.* 89(8) (1989) 1861.
13. Khiew P.S., Radiman S., Huang N.M., Soot Ahmad M.D., Nadarajah K., *Mater. Lett.* 59 (2005) 989.
14. Ma Y., Qi L., Ma J., Cheng H., *Langmuir* 19 (2003) 4040.
15. Vogel W., *Langmuir* 16 (2000) 2032.
16. Nistor L.C., Mateescu C.D., Birjega R., Nistor S.V., *Appl. Phys. A* 92 (2008) 295.
17. Vijai Anand K., Karlchinnu M., Mohankumar R., Mohan R., Jayavel R., *Appl. Surf. Sci.* 255 (2009) 8879.
18. Vijai Anand K., Karlchinnu M., Mohankumar R., Mohan R., Jayavel R., *J. Alloys Compds.* 496 (2010) 665.
19. Vijai Anand K., Mohan R., Mohankumar R., Karlchinnu M., Jayavel R., *Int. J. Nanoscience* 10 (2011) 487.
20. Vijai Anand K., Mohan R., Mohankumar R., Karlchinnu M., Jayavel R., *J. Exp. Nanoscience* 9 (2014) 261.
21. Naskar M.K., Patra A., Chatterjee M. *J. Colloid Interface Sci.* 297 (2006) 271.
22. Hoa T.Q., Vu L.V., Canh T.D., Long N.N., *J. Phys.: Conf. Ser.* 187 (2009) 012081.
23. Chen S., Liu W., *Mater. Res. Bull.* 36 (2001) 137.
24. Gao J., Lu C., Lu X., Du Y., *J. Mater. Chem.* 17 (2007) 4591.
25. Zhang Y., Wang S., Qian Y., Zhang Z., *Solid State Sci.* 8 (2006) 462.
26. Chen S., Liu W., *Langmuir* 15 (1999) 8100.
27. Sugunan A., Warad HC., Boman M., Dutta J., *J. Sol-Gel Sci. Technol.* 39 (2006) 49.
28. Tang H., Yan M., Zhang H., Xia M., Yang D., *Mater. Lett.* 59 (2005) 1024.
29. El-Kemary M., El-Shamy H. *J. Photochem. Photobio. A: Chemistry* 205 (2009) 151.
30. Remadevi B.S., Raveendran R., Vaidyan A.V., *Pramana*, 68 (2007) 679.

(2016) ; <http://www.jmaterenvirosci.com>